

# INTERNATIONAL SOCIETY FOR SOIL MECHANICS AND GEOTECHNICAL ENGINEERING



*This paper was downloaded from the Online Library of the International Society for Soil Mechanics and Geotechnical Engineering (ISSMGE). The library is available here:*

<https://www.issmge.org/publications/online-library>

*This is an open-access database that archives thousands of papers published under the Auspices of the ISSMGE and maintained by the Innovation and Development Committee of ISSMGE.*

# Stresses and Strains in Sand in Axially Symmetrical Case

## Déformations de Sable dans la Cellule Triaxiale

A. KÉZDI and  
GY. HORVÁTH Department of Geotechnique, Technical University of Budapest, Hungary

**SYNOPSIS** Using a specially transformed triaxial testing device which can be used to work along any prescribed stress path (either stress or strain control), tests were performed to investigate the strains and volume changes in sand. A given homogeneous initial condition has been established with a prescribed phase composition ( $w < w_{opt}$ ). The rate of loading was the same for all tests. During loading, strains, volume changes and pore pressures were measured and the character of the variations in the different stages of the test observed. In the process which leads to failure, the soil is subjected to several characteristic critical conditions; these limits could be clearly determined.

### Introduction

The shear strength and the shear strain of sand have been investigated in great details for many years; the problem can be considered as solved for daily practice: factors affecting shear strength, laws of volume change, the concept of critical density are known. In general tests are carried out either with completely dry or with fully saturated soil samples, because of lack of cohesion in such instances. This is usually motivated by the fact that sand dries out easily and, in case of inundation, becomes easily saturated, therefore cohesion which is present in the three phase state, ceases. The authors intended to broaden the field of investigation and to use samples having three phases. They carried out triaxial tests with sand; the purpose of the research was to furnish the physical basis to the detailed investigation of failure mechanism of soil masses, covering the whole process of failure development. Here the first results of these study are presented.

### Material and method used in the tests

The grain size distribution curve of the test sand and its compaction curve obtained by the modified Proctor test are given in Fig. 1. Samples having various phase composition with 20 cm height and a diameter of 10 cm were subjected to an axially symmetrical stressed state, in a Wykeham Farrance Engg. Ltd/England, WF 11001 apparatus. To measure the shear strains the triaxial apparatus had to be modified in order to make it suitable to measure the volume change, the vertical and radial strains, for any stress path.

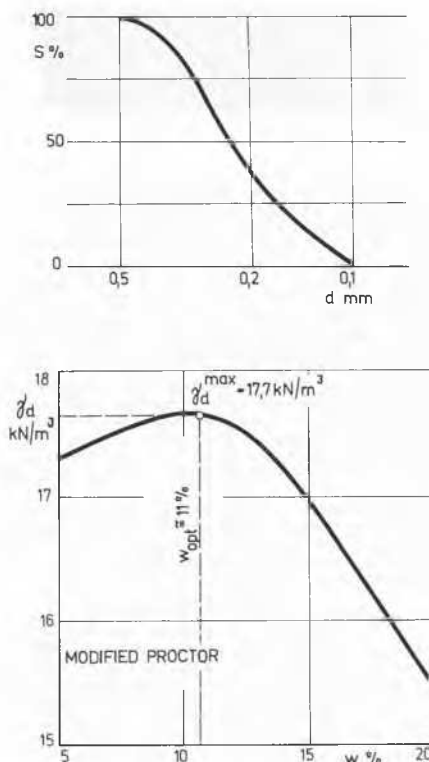


Fig. 1. Grading curve and compaction curve of sand tested

The testing equipment is shown in Fig. 2. The modified piston and the measuring devices are clearly visible; a detailed description will be given elsewhere.



Fig. 2. Modified triaxial cell

Stresses were increased by a constant rate of loading. Taking into account the coefficient of permeability  $k \sim 0,002$  to  $0,006 \text{ cm s}^{-1}$ , the system may be considered as open. Tests were carried out by using several different stress paths. First, a hydrostatic stress  $\sigma_1 = \sigma_2 = \sigma_3 = p_0$  was applied /Fig. 3 line I./, up to  $p_0 = 200 \text{ kN/m}^2$  then  $\sigma_1$  was increased and  $\sigma_2 = \sigma_3$  kept constant. In the other type /Fig. 3 line II/, in order to simulate the states of stress beneath an uniformly loaded circular area, in the first part the  $K_0$  - state was established then the sample brought to failure. The typical shape of the curve giving the corresponding volume changes is shown in Fig. 3, below the diagram of stress circles.

The homogeneity of the sample was ensured by uniform compaction, its dry bulk density being  $\gamma_d = 16,3 \text{ kN/m}^3$ , wet bulk density  $17,8 \text{ kN/m}^3$ , moisture content  $w = 8$  per cent, degree of compaction  $T_{\gamma} = 0,92$ .

On the diagram of the volume change /Fig. 3./, point O represents the starting position. Section O-1 corresponds to the increase of the hydrostatic stress / stress path No. I.,  $\sigma_1 = \sigma_2 = \sigma_3$ /. Reading the value  $\sigma = 200 \text{ kN/m}^2$  /point 1/; specific volume change  $\beta_1$ /, hence forward, only  $\sigma_1$  was increased. The specific volume change is compression in the range 1 - 3 and up to point 2, it is linear. Beyond point 2, the relationship is characterized by a curve. It is probable that at this stage plastic defor-

mations occur in the sample. The length of range 2 - 3 depends on the phase composition; in moist, dense state sometimes point 2 coincided with point 3. It was an important observation that in such cases failure was always associated with the development of a definite sliding phase; in other instances by plastic flow. Beyond point 3 the shear strain increased, the sample became looser and failure occurred. The highest vertical principal stress /point 4,  $\sigma_1^{max}$ / was considered as failure stress.

The test carried out according to stress path II, served first to the determination of the coefficient of earth pressure at rest  $K_0$ , then stress states corresponding to different conditions were investigated. In general, the variation of volume change  $\beta$  followed the same character, however, the absolute values of the volume change for the same initial phase composition were smaller. /Fig. 3./

The calculations were carried out with a computer Hewlett-Packard 9830; the prescribed stress path was ensured by automatic control.

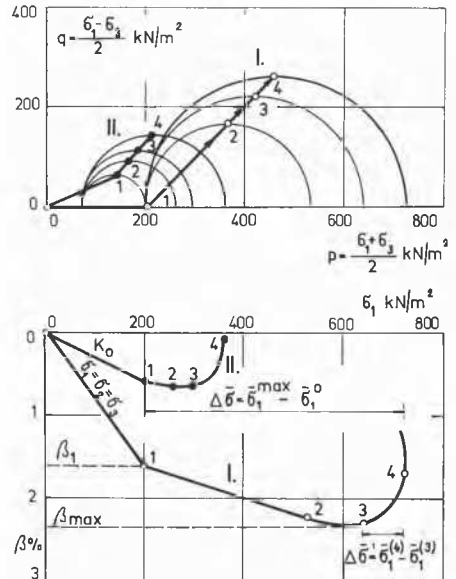


Fig. 3. Typical test result; top: stress paths; bottom: volume changes

Test results

Fig. 4. gives, in a triangular chart which displays the phase composition of the soil by volume  $s = V_s/V$ ,  $v = V_w/V$ ,  $l = V_a/V$ , with partial volume of the solids, water and air, respectively/ the volume changes for the ranges  $0 - 1$  /on triangle a/ and for  $1 - 2$  /on triangle b/.  $\beta_1$  belongs to the hydrostatic stress  $p_0 = 200 \text{ kN/m}^2$ . Here, and in the following triangular charts the marked part of the diagram will be used. The volume change decreases with the increase in density, but the effect of changes in moisture content is smaller. There exists for any value  $s =$  constant a critical value  $v$ , where the Volume change is smallest.

Curves of quite similar character were obtained for the range  $1-2$  / $\beta_2$  /, a volume change which occurred when the effective principal stress  $\sigma_1 = 200 \text{ kN/m}^2$  was increased to  $\sigma_1 = 500 \text{ kN/m}^2$ , and  $\sigma_2 = \sigma_3$  remained constant  $l = 200 \text{ kN/m}^2$ .

Diagram a shows the stress increment which was required to produce failure /see Fig. 3/. It is interesting to note that the peak points /i.e. the optimum phase compositions for strength/ are located on a straight line corresponding to  $S = 0,46$ . This is in accordance with the experience that the highest strength can be obtained at a water content which is lower than the Proctor optimum.

$\beta_3$  % the specific volume change in the range  $3 - 4$  is expansion /diagram b in Fig. 4/ with regard to the condition marked 3. In the tests, the points representing the phase composition of the sample in the states  $1 - 2 - 3 - 4$  changed along a straight line, because during the test no water left the sample. If we calculate the angle of internal friction from the formula

$$\sin \phi = \frac{\frac{\sigma_1^{\max} - \sigma_1^0}{\sigma_1^{\max} + \sigma_1^0}}{\frac{\sigma_1^{\max} - \sigma_1^0}{\sigma_1^{\max} + \sigma_1^0}}$$

and plot the  $\phi$  values on the triangular / $s, v, l$ / chart, we obtain  $\phi =$  constant lines /see Fig. 4, chart b/. The decisive factor is density; the change in water content is of minor importance.

The second type of test /stress path II, in Fig. 3/ served, first, to determine of the coefficient of earth pressure at rest. Up to now, the number of tests is not sufficient to plot  $K_0$  values in a triangular diagram, only the curve in Fig.5. can be given. For our present purpose it was more important to gain insight into the process of failure, and to investigate the influence of the stress path and of the phase composition on the failure.

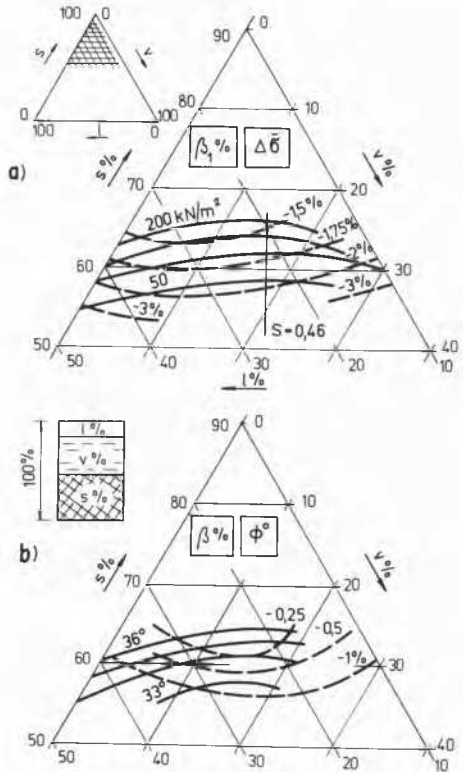


Fig. 4. Test results as functions of phase composition

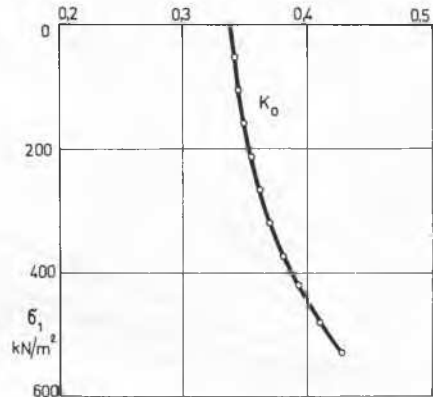


Fig. 5. Variation of the coefficient  $K_0$  with the major principal stress  $\sigma_1$

In the case of a given initial phase composition /here  $s = 61,5 \%$ ,  $v = 12,5 \%$ /, the general character of the stress path, of the deformation diagrams and of the volume change is shown in Fig. 6.

The limits of the different behaviours could be clearly located: 0 - 1 at rest condition, 1-2 continuing densification, 2-3 radial displacement, point 3 critical point, where loosening starts, point 4 complete failure. For the above mentioned phase composition, the test results are given in Fig. 7; here in the coordinate system /  $\sigma_1$ ,  $\sigma_3$  / the stressed state at these limits are plotted.

The coefficient of earth pressure at rest / $K_0 = \tan \alpha_0 = \sigma_3 / \sigma_1$ / is 0,34; but the limit of the elastic behavior could not be given by a constant ratio of the principal stresses because of the cohesion at this phase composition. Line 3 has the same character.

There were difficulties in determining the line 4 which corresponds to the total failure. For technical reasons, the failure state could not be reached in every case /particularly in the loose state/ and, which is more important, the failure occurred in a rather peculiar way. The initial densification was followed, as shown in Fig. 3, by a loosening /range 3 - 4/, then another densification and loosening occurred, thus, the volume change at failure is indeterminate. Based on the first plastic state, the approximate line 4 could be given.

Further tests, to be carried out according to the stressed states beneath a uniformly loaded circular area, will furnish the base to the investigation of the failure mechanism in a soil mass.

Fig. 6. Stress path, stress-strain diagram and volume changes in a typical test

Fig. 7. Lines representing states 1-2-3-4 obtained by various stress paths

